

## Shape isomerism and shape coexistence effects on the Coulomb energy differences in the $N = Z$ nucleus $^{66}\text{As}$ and neighboring $T = 1$ multiplets

G. de Angelis,<sup>1</sup> K. T. Wiedemann,<sup>2,\*</sup>† T. Martinez,<sup>1,‡</sup> R. Orlandi,<sup>1,§</sup> A. Petrovici,<sup>3</sup> E. Sahin,<sup>1</sup> J. J. Valiente-Dobón,<sup>1</sup> D. Tonev,<sup>4</sup> S. Lunardi,<sup>5</sup> B. S. Nara Singh,<sup>6</sup> R. Wadsworth,<sup>6</sup> A. Gadea,<sup>7</sup> K. Kaneko,<sup>8</sup> P. G. Bizzeti,<sup>9</sup> A. M. Bizzeti-Sona,<sup>9</sup> B. Blank,<sup>10</sup> A. Bracco,<sup>11</sup> M. P. Carpenter,<sup>12</sup> C. J. Chiara,<sup>13,||</sup> E. Farnea,<sup>5</sup> A. Gottardo,<sup>1</sup> J. P. Greene,<sup>12</sup> S. M. Lenzi,<sup>5</sup> S. Leoni,<sup>11</sup> C. J. Lister,<sup>12</sup> D. Mengoni,<sup>5</sup> D. R. Napoli,<sup>1</sup> O. L. Pechenaya,<sup>13,¶</sup> F. Recchia,<sup>5</sup> W. Reviol,<sup>13</sup> D. G. Sarantites,<sup>13</sup> D. Seweryniak,<sup>12</sup> C. A. Ur,<sup>5</sup> and S. Zhu<sup>12</sup>

<sup>1</sup>Laboratori Nazionali di Legnaro dell' INFN, I-35020 Legnaro (Padova), Italy

<sup>2</sup>Universidade de São Paulo, São Paulo, P.O. Box 66318, Brazil

<sup>3</sup>Horia Hulubei National Institute for Physics and Nuclear Engineering, R-077125 Bucharest-Magurele, Romania

<sup>4</sup>Institute for Nuclear Research and Nuclear Energy, BAS, 1784 Sofia, Bulgaria

<sup>5</sup>INFN Sezione di Padova and Dipartimento di Fisica, Università di Padova, I-35131 Padova, Italy

<sup>6</sup>University of York, York, YO10 5DD, United Kingdom

<sup>7</sup>IFIC, CSIC–University of València, E-46100 València, Spain

<sup>8</sup>Department of Physics, Kyushu Sangyo University, Fukuoka 813-8503, Japan

<sup>9</sup>Dipartimento di Fisica, Università di Firenze and INFN Sezione di Firenze, I-50019 Sesto Fiorentino (Firenze), Italy

<sup>10</sup>CEN Bordeaux-Gradignan, F-33175 Gradignan, France

<sup>11</sup>INFN Sezione di Milano and Dipartimento di Fisica, Università di Milano, I-20133 Milano, Italy

<sup>12</sup>Argonne National Laboratory, Argonne, Illinois 60439, USA

<sup>13</sup>Department of Chemistry, Washington University, St. Louis, Missouri 63130, USA

(Received 10 February 2012; revised manuscript received 22 February 2012; published 20 March 2012)

Excited states of the  $N = Z = 33$  nucleus  $^{66}\text{As}$  have been populated in a fusion-evaporation reaction and studied using  $\gamma$ -ray spectroscopic techniques. Special emphasis was put into the search for candidates for the  $T = 1$  states. A new  $3^+$  isomer has been observed with a lifetime of 1.1(3) ns. This is believed to be the predicted oblate shape isomer. The excited levels are discussed in terms of the shell model and of the complex excited Vampir approaches. Coulomb energy differences are determined from the comparison of the  $T = 1$  states with their analog partners. The unusual behavior of the Coulomb energy differences in the  $A = 70$  mass region is explained through different shape components (oblate and prolate) within the members of the same isospin multiplets. This breaking of the isospin symmetry is attributed to the correlations induced by the Coulomb interaction.

DOI: [10.1103/PhysRevC.85.034320](https://doi.org/10.1103/PhysRevC.85.034320)

PACS number(s): 21.60.Cs, 23.20.Lv, 25.70.Hi, 27.50.+e

### I. INTRODUCTION

Isospin symmetry, the exchange symmetry between protons and neutrons, with its associated isospin quantum number, is one of the basic concepts in nuclear physics. Analog states belonging to the same isobaric multiplet (in which we refer to both isospin  $T = 1/2$  and  $T = 1$  multiplets) are nearly identical, their differences originating from isospin non-conserving forces such as the Coulomb interaction. The differences in the excitation energies of the isobaric analog

states, called Coulomb energy differences (CED), have been widely used in order to investigate, through the Coulomb effects, the microscopic structure of atomic nuclei. They have provided information on nucleon alignment, on the evolution of the nuclear radii, and on specific terms of the residual interaction. More details can be found in Refs. [1,2] and in references therein. In such studies it is generally assumed that all nuclei in the same isobaric triplet have identical shape and that the Coulomb interaction can be treated as a perturbation [1,3,4]. The polarization effects induced through Coulomb interaction by the valence nucleons are therefore ignored. Due to the almost charge independence of the strong force, those effects are generally small but they can become significant in nuclear regions where two competing mean-field shapes coexist at low excitation energies. In these cases the modification induced to the orbitals by the Coulomb field of the valence particles can result in a modification of the energetically favored shape, eventually causing a further breaking of the isospin symmetry [5]. Moreover, because prolate and oblate shapes coexist at low excitation energy, shape isomerism is expected. This is indeed the case of the mass  $A = 70$  region where large shell gaps exist at both prolate and oblate shapes for  $N = Z = 34$  and 36–38. Here small

\*Present address: Harvard School for Engineering and Applied Sciences, Cambridge, MA, USA.

†Present address: University of Arizona, Ecology and Evolutionary Biology, Tucson, AZ, USA.

‡Present address: Centro de Investigaciones Energéticas, MedioAmbientales y Tecnológicas, CIEMAT, Madrid, Spain.

§Present address: Instituto de Estructura de la Materia-CSIC, Madrid, Spain.

||Present address: Department of Chemistry, University of Maryland, Maryland 20742, USA.

¶Present address: Department of Radiation Oncology, Washington University, St. Louis, Missouri, USA.

modifications in the Fermi surface induced by the Coulomb interaction can cause rapid changes in the nuclear shape, altering the mixing of prolate and oblate components, and may lead to different shapes in the ground-state configurations of nuclei belonging to the same isospin multiplet. Moreover, since such nuclei lie in the mass region where stellar nucleosynthesis takes place, changes in deformation of close-lying nuclei, with the possible existence of long-living shape isomers, can significantly affect the proton-capture rates and therefore the rp-process path [6].

CED in isobaric triplets (defined in Ref. [3] as the difference between the excitation energies of the lowest  $T = 1$  states in the  $N = Z T_z = 0$  and  $N = Z + 2 T_z = 1$  members of the isobaric multiplet) generally show an increasing trend as a function of nuclear spin (see Fig. 2 of Ref. [3]), a behavior which has been attributed to the effect of the Coriolis antipairing on the nucleon-nucleon correlations [3]. Decreasing or almost flat behavior of the CED has been observed for  $A = 70$  and  $78$  and for the first excited state of  $A = 66$  [3,7]. The unexpected negative trend of the CED found for the  $^{70}\text{Br}$ - $^{70}\text{Se}$  pair has been attributed to the Thomas-Ehrman shift [7]. A different interpretation based on the shape evolution of those nuclei with increasing angular momentum has been suggested in Ref. [3]. In the same reference, an almost flat behavior of the CED is observed for the  $A = 78$   $^{78}\text{Y}$ - $^{78}\text{Sr}$  pair and is interpreted as due to the stiffness of those nuclei caused by the large deformed shell gap at  $N = Z = 38$ .

In this paper, we show that all these different behaviours of the CED can be attributed to the polarization effects of the valence particles through the isospin-breaking Coulomb interaction. The modification induced on the proton single-particle energies causes changes in the mixing of competing shapes with strong effects on the CED. In order to help clarify the relation between CED and shape changes we have investigated the excited structure of the  $N = Z = 33$   $^{66}\text{As}$ , a nucleus where the coexistence of different shapes is expected. The new experimental data are used, along with nuclear model calculations, to review the CED systematics in the nuclei of the  $A = 70$  mass region.

## II. EXPERIMENT

The  $^{66}\text{As}$  nucleus was produced in the fusion evaporation reaction  $^{40}\text{Ca}(^{32}\text{S}, \alpha pn)^{66}\text{As}$ . The 90-MeV  $^{32}\text{S}$  beam, pulsed with a frequency of 12 MHz, was provided by the ATLAS accelerator at Argonne National Laboratory. The target was made of a  $550 \mu\text{g}/\text{cm}^2$  thick foil of  $^{40}\text{Ca}$ , evaporated onto a Au backing with a thickness of  $10 \text{ mg}/\text{cm}^2$ , and covered by a  $30 \mu\text{g}/\text{cm}^2$  thick Au front layer to preserve it from oxidation. The emitted  $\gamma$  rays were detected by the Gammasphere array [8]. The high selectivity required for the identification of the different reaction channels was obtained with the employment of MicroBall [9] and NeutronShell [10], the latter array replacing the forward five Gammasphere rings. Each reaction channel was selected according to the number of evaporated charged particles (protons and  $\alpha$  particles) and neutrons. Data were sorted into two- and three-dimensional matrices under the conditions of detecting one  $\alpha$  particle and one proton in MicroBall and one neutron in NeutronShell. Examples of gated

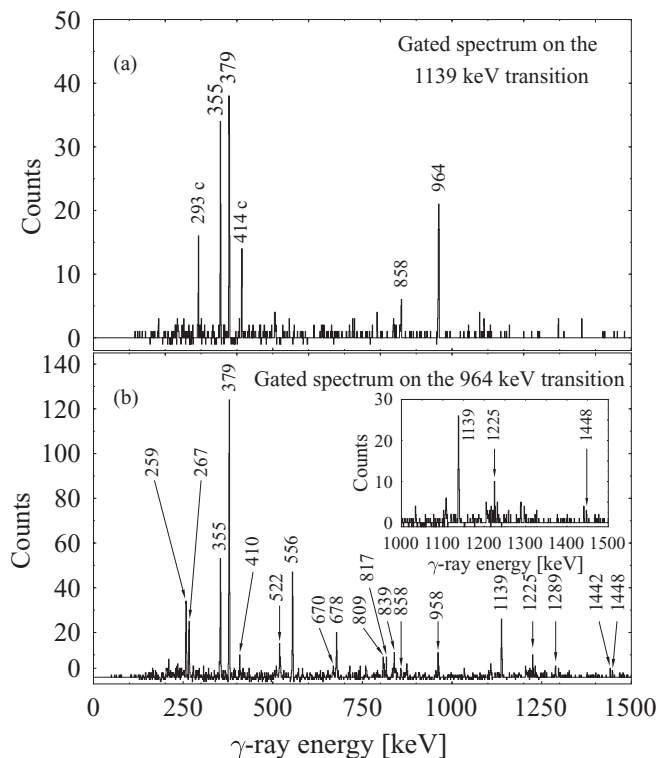


FIG. 1.  $\gamma$ -ray spectra gated on the  $\alpha pn$  reaction channel and on the 1139-keV ( $5^+ \rightarrow 3^+$ ) (a) and on the 964-keV  $2^+ \rightarrow 0^+$  transitions (b). The inset shows part of the spectrum gated on the 964-keV line. Labels of contaminant peaks (from  $^{45}\text{Ti}$  produced in the  $^{32}\text{S} + ^{16}\text{O}$  reaction) are followed by a “c.”

$\gamma$ -ray spectra after selecting the  $^{66}\text{As}$  reaction channel with charged particle and neutron conditions are shown in Fig. 1.

## III. RESULTS

The level scheme of  $^{66}\text{As}$ , determined in this work, is presented in Fig. 2. The levels are grouped, depending on their decay to the 837-keV  $1^+ \rightarrow 0^+$  or the 964-keV  $2^+ \rightarrow 0^+$ , in  $T = 0$  and  $T = 1$  structures. Previous information about the excited states of  $^{66}\text{As}$  following the de-excitation of the  $T = 0$ ,  $I^\pi = 9^+$  isomeric state [ $t_{1/2} = 8.2(5) \mu\text{s}$ ] is reported in Ref. [11]. The level scheme of Fig. 2 shows a complex structure dominated by the  $T = 0$  states. We confirm the levels previously identified through the decay of the tentatively assigned  $9^+$  isomer [11], which are not observed in the present data due to the prompt time conditions. In addition, we observe more than 20 new  $\gamma$  transitions extending the level scheme up to an excitation energy of  $\approx 4.8 \text{ MeV}$  and  $I^\pi \geq (7^+)$ . In coincidence with the 837-keV transition we observe several decay branches partially linked to the previously identified level structure. A 506-keV transition defines a level at 1.343 MeV, which decays to the  $2^+$  state at 0.964 MeV through a 379-keV  $\gamma$  transition and to the  $3^+$  state at 1.231 MeV through a 112-keV line, which is unobserved due to the absorption of the Microball detectors. With increasing spin and excitation energy a more complex structure dominates, which de-excites, through several transitions, to the states at 1.231 and 1.343 MeV as well as to the  $2^+$  level at 0.964 MeV.



TABLE I. Gamma energies ( $E_\gamma$ ), relative intensities ( $I_\gamma$ ), angular distribution coefficients (A2 and A4), and ADO ratios ( $R_{\text{ADO}}$ ) for the transitions observed in  $^{66}\text{As}$ . For the ADO ratios, extracted by adding data from the three detector rings, the transitions used as gates are indicated. The proposed spin-parity assignments for the levels involved are also given.

$E_\gamma(\text{keV})^a$	$I_\gamma$	A2	A4	$R_{\text{ADO}}$	$I_i^\pi$	$I_f^\pi$
112	6 (2) <sup>b</sup>				3 <sup>+</sup>	3 <sup>+</sup>
259	13 (1)			0.6(2) <sub>964</sub>	(3)	2 <sup>+</sup>
267	8 (1)			1.0(4) <sub>964</sub>	3 <sup>+</sup>	2 <sup>+</sup>
354	4 (2)				(4 <sup>+</sup> )	4
355	20 (3)			1.0(4) <sub>964</sub>	(7 <sup>+</sup> )	(5 <sup>+</sup> )
379	42 (3)	-0.22(11)	0.20(19)	0.5(1) <sub>964</sub>	3 <sup>+</sup>	2 <sup>+</sup>
394	44 (3)	0.21(8)	0.0(1)	1.1(3) <sub>670</sub>	3 <sup>+</sup>	1 <sup>+</sup>
410	5 (2)				4	3 <sup>+</sup>
506	7 (1)				3 <sup>+</sup>	1 <sup>+</sup>
522	15 (3)			1.9(5) <sub>394</sub>	4	3 <sup>+</sup>
556	17 (2)			0.5(2) <sub>964</sub>	4	3 <sup>+</sup>
670	19 (2)	0.32(14)	-0.1(2)	1.0(2) <sub>394</sub>	5 <sup>+</sup>	3 <sup>+</sup>
678	7 (2)					2 <sup>+</sup>
729	3 (2)				(5 <sup>+</sup> )	4
809	4 (2)					3
815	4 (2)					5 <sup>+</sup>
817	4 (1)					4
837	71 (3)	-0.27(6)	0.0(1)	0.7(1) <sub>394</sub>	1 <sup>+</sup>	0 <sup>+</sup>
839	8 (2)				(5 <sup>+</sup> )	
858	3 (2)					
958	3 (1)				(4 <sup>+</sup> )	3 <sup>+</sup>
964	100	0.20(8)	0.1(1)		2 <sup>+</sup>	0 <sup>+</sup>
1006	5 (1)					5 <sup>+</sup>
1033	4 (2)					4
1089	3 (1)					
1139	16 (3)			0.9(4) <sub>964</sub>	(5 <sup>+</sup> )	3 <sup>+</sup>
1225	4 (2)				(4 <sup>+</sup> )	(2 <sup>+</sup> )
1289	4 (1)					2 <sup>+</sup>
1235	4 (2)					5 <sup>+</sup>
1442	2 (1)					3 <sup>+</sup>
1448	2 (1)				(6 <sup>+</sup> )	(4 <sup>+</sup> )

<sup>a</sup>Uncertainties are within 1 keV.

<sup>b</sup>The intensity for this transition (unobserved due to the absorption of the Microball detectors) is extracted from the intensity balance of the 506, 379 keV and 394, 267 keV transitions in the spectrum gated by the 556-keV line.

gating on transitions above and below the 3<sup>+</sup> isomeric state, the centroid of the time distribution undergoes a shift with respect to the prompt position, equivalent to the lifetime of the state; by reversing the ordering of the  $\gamma$ -ray gates, the time distribution shifts by the same amount in the opposite direction (Fig. 3). The dependence of the centroid shift on the signal amplitude, which becomes important at lower energies, was determined from the study of prompt  $\gamma$ -ray transitions and taken into account in the analysis. Details of the method are reported in Ref. [12]. From the experimentally determined lifetime and branching ratios,  $B(E2; 3_2^+ \rightarrow 1^+) = 2.9(8) e^2 \text{fm}^4$  is extracted.

#### IV. DISCUSSION

$^{66}\text{As}$  belongs to a transitional mass region which includes nuclear systems ranging from the weakly deformed nuclei at the shell closures  $N = Z = 28$  to the strongly deformed nuclei around  $^{80}\text{Zr}$ . The low single-particle level density as well as the proximity of the  $g_{9/2}$  intruder orbit to the Fermi surface

for protons and neutron favors the stabilization of different (oblate and prolate) shapes at similar excitation energy. The proximity of levels with opposite sign of the quadrupole moment and therefore with small overlap of the wave functions can determine the formation of shape isomers. A low-lying 3<sup>+</sup> isomeric state has been recently predicted in  $^{66}\text{As}$  by shell-model (SM) calculations [13] due to the prolate and oblate shape coexistence at low excitation energy. It is expected to be oblate, in contrast to the prolate shape for the other low-lying states. Furthermore, its decay to the 1<sup>+</sup> level is predicted to be strongly hindered [ $B(E2) = 1.3 \text{ W.u.}$ ] compared to other  $E2$  transitions between the  $T = 0$  states, which are calculated to be an order of magnitude larger. The value we obtain for the transition matrix element  $B(E2; 3_2^+ \rightarrow 1^+)$  of 0.18(5) W.u. is in reasonable agreement with the expectation based on shape isomerism. It is 70 times smaller than the  $B(E2; 3^+ \rightarrow 1^+)$  value observed in the  $N = Z = 31$  nucleus  $^{62}\text{Ga}$  [15,16], where similar calculations do not predict different deformed shapes for the 3<sup>+</sup> level with respect to the yrast 1<sup>+</sup> state [13].

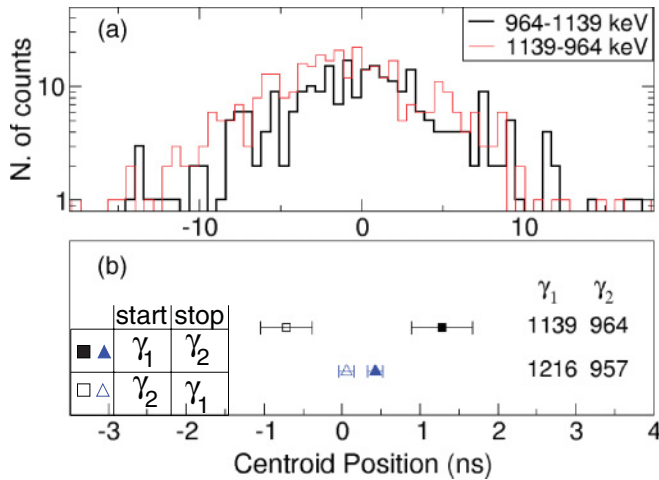


FIG. 3. (Color online) (a) Relative-time distributions for the 964- and 1139-keV  $\gamma$ -ray pair. (b) Centroids of the relative time distributions for two different pairs of  $\gamma$  transitions in direct and reverse order. Delayed coincidences across the  $3^+$  isomeric state are shown in the upper part of the figure; prompt coincidences, from  $^{66}\text{Ge}$ , are shown in the lower part.

### A. Shell-model calculations

Shell-model calculations for  $^{66}\text{As}$  using the JUN45 interaction have also been recently reported in Ref. [14] and compared with the known data at that time. However, not all calculated states were shown in that work, and hence we have also performed SM calculations (see Ref. [14] for details) in the  $fp$ g model space using the JUN45 interaction. Figure 4 shows the results of these calculations along with the experimental levels. For the  $T = 0$  states, the calculations reproduce well the experimental energy levels. All low-lying states are mainly based on  $f_{5/2}$ ,  $p_{3/2}$ , and  $p_{1/2}$

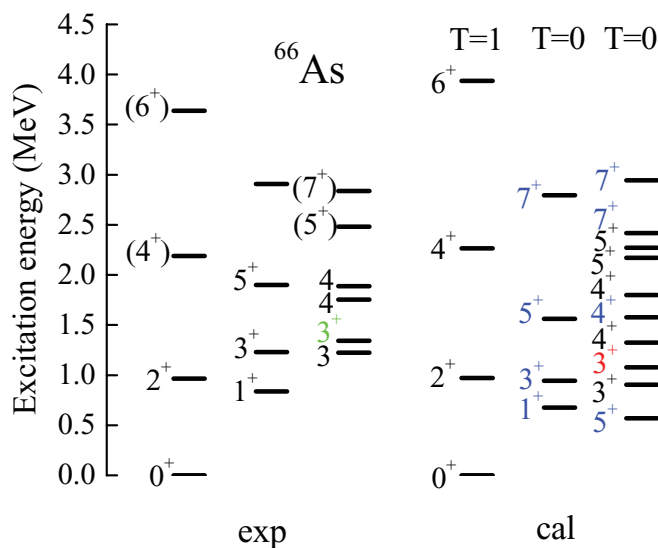


FIG. 4. (Color online) Comparison of the experimental and calculated energy levels (JUN45) for  $^{66}\text{As}$ . The isomeric  $3^+$  state is shown in red (gray).  $T = 0$  states connected by large  $E2$  transitions are reported separately.

configurations. The level sequence of the three calculated  $3^+$  states corresponds well to the experimental ones. For the third  $3^+$  state a large positive spectroscopic quadrupole moment  $Q_s = +30 e \text{ fm}^2$  is predicted, corresponding to an oblate shape. This state has a different structure to all other low-lying states, which have negative  $Q_s$  values, implying a prolate shape. As a consequence, the decay from the third  $3^+$  state to the lower lying states is strongly hindered. For example, the corresponding  $B(E2 : 3^+ \rightarrow 1^+)$  strength is only  $B(E2) = 1.8 \text{ W.u.}$ , which is consistent with the value reported (1.3 W.u.) in Ref. [13]. However, the experimental data indicate a smaller value of 0.18 W.u.. The two experimentally observed  $J = 4$  levels compare very reasonably in terms of excitation energy with the  $T = 0, 4^+$  calculated states. Four  $5^+$  states are predicted by the calculations, all based on  $fp$  configurations. As already reported in Ref. [14], the SM predicts the yrast  $5^+$  isomeric state (not observed in our data due to the isomerism) at lower excitation energy compared to the data [11]. Two of the experimentally identified  $5^+$  levels are in reasonable agreement with the predicted states. The  $5^+$  state observed at 2.5 MeV has a very fragmented decay path, which is consistent with the almost vanishing quadrupole moment predicted for this state. Three excited  $7^+$  states are predicted and partially observed, two of them based on  $fp$  configurations and one involving also a proton-neutron pair excited into the intruder  $g_{9/2}$  orbit. In Fig. 4 the candidates for the  $T = 1$  states are also reported. The calculated level energies compare reasonably well with the experimental excitation energies up to the ( $4^+$ ) state overestimating the ( $6^+$ ) level probably due to the limited configuration space used in the calculations. In associating those levels with the  $T = 1$  states it is interesting to discuss their branching ratios. The  $2^+$  state at 0.964 MeV decays only to the  $0^+$  ground state. A possible branch to the  $1^+$  level is below our sensitivity limit. The ( $4^+$ ) state at 2.189 MeV de-excites to the  $2^+$  (57%) and to the  $3^+$  (43%) states. The proposed ( $6^+$ ) level at 3.637 MeV decays only to the lower lying  $4^+$  level. This behavior is quite different from the lighter  $N = Z$  odd-odd nuclei in the  $fp$  shell up to  $^{62}\text{Ga}$  [16] and is more similar to that observed for the heavier nuclei  $^{70}\text{Br}$  [17] and  $^{74}\text{Rb}$  [18]. In the case of the lighter odd-odd  $N = Z$  nuclei the decay of the  $T = 0$  states is dominated by strong isovector  $M1$  transitions, which overcome the isoscalar stretched  $E2$  decays, reaching strengths up to  $B(M1 : 1^+ \rightarrow 0^+) \approx 4\mu_n^2$  in  $^{54}\text{Co}$  [19]. Such  $M1$  transitions have been associated with quasideuteron configurations [20] described as the coupling between an inert even-even  $N = Z$  core and one valence proton and one valence neutron occupying the same  $j = l + 1/2$  orbital. As demonstrated in Ref. [20], when the orbital angular momentum and the spin are aligned the spin and orbital components of the isovector  $M1$  transition operator are summed up in phase, resulting in large  $M1$  transition strength. A different situation arises in cases where the two valence nucleons are occupying the same  $j = l - 1/2$  orbital. Here the orbital and spin parts of the  $M1$  operator partially cancel and the  $M1$  matrix elements become small. Since  $^{66}\text{As}$  is situated in the upper part of the  $fp$  shell, low-lying excitations mainly involve the  $p_{3/2}(j = l + 1)$  and the  $f_{5/2}(j = l - 1)$  orbitals. The former, in the quasideuteron description, will favor strong isovector  $M1$  transitions while the latter will

suppress them. The small  $M1$  branches observed in  $^{66}\text{As}$  are therefore expected [16] and can be associated with the large contribution of the  $f_{5/2}$  orbital in the wave functions of the low-lying excitations. This is also consistent with the small  $M1$  branches observed in the heavier  $N = Z$  odd-odd nuclei  $^{70}\text{Br}$  and  $^{74}\text{Rb}$ , which have low-lying excitations dominated by the  $f_{5/2}$  orbit, and with the larger  $M1$  branches observed in the lighter  $^{62}\text{Ga}$ , where the low-lying excitations will have a larger  $p_{3/2}$  content.

### B. Complex excited Vampir calculations

To investigate possible shape coexistence phenomena the excited  $T = 1$  states of  $^{66}\text{As}$ , and other nuclei of interest, have been calculated using the complex excited Vampir model [21]. This model has been successfully applied for a microscopic description of analog states in the  $A = 70$  mass region [22]. It takes into account oblate-prolate shape coexistence and mixing, allowing a unified description for low- and high-spin states including neutron-proton pairing correlations in both the  $T = 1$  and  $T = 0$  channels. We have calculated, using the isospin-symmetric  $G$  matrix based on the Bonn A potential and the Coulomb interaction between valence protons, the lowest positive-parity states for the  $A = 70$ ,  $^{70}\text{Br}$ - $^{70}\text{Se}$ , and  $A = 66$ ,  $^{66}\text{As}$ - $^{66}\text{Ge}$ , pairs. First, the Vampir solutions have been obtained by representing the one-symmetry-projected Hartree-Fock-Bogoliubov determinant optimal for the yrast states. Then, the excited Vampir approach was used to construct additional excited states by independent variational calculations. Finally, for each considered spin the residual interaction between the various configurations was diagonalized. The neutron single-particle energies for the adopted model space (in units of the oscillatory energy  $\hbar\omega = 41.2A^{-1/3}$ ) are reported in Table II. For details of the calculations see Ref. [22].

The results obtained for the  $A = 70$  nuclei show the presence of a strong competition between configurations based on oblate and prolate quadrupole deformations [22]. In  $^{70}\text{Br}$ , the ground state is predominantly prolate and the oblate (prolate) component is found to be 36% (64%), 41% (59%), 41% (58%), 20% (80%) for the first  $0^+$ ,  $2^+$ ,  $4^+$ , and  $6^+$  states, respectively. For  $^{70}\text{Se}$ , the calculation predicts a predominantly oblate ground state, in good agreement with the recent measurement of Ref. [23], and the oblate (prolate) component is found to be 57% (42%), 59% (41%), 64% (36%), and 39% (61%) for the respective analog states. By using  $e_\pi = 1.2$  and  $e_\nu = 0.2$  for the effective proton and neutron charges, respectively [24], the model provides  $B(E2, I \rightarrow I - 2)$  values of 492, 713, and 779  $e^2 \text{fm}^4$  for the  $E2$  transitions de-exciting the  $I^\pi = 2^+$ ,  $4^+$  and  $6^+$  states. These are in reasonable agreement with the experimental values, i.e., 342(19), 370(24) and 530(96)  $e^2 \text{fm}^4$ , of Ref. [23]. The calculated spectroscopic quadrupole moment

TABLE II. Neutron single-particle energies (in oscillator energy units).

$(1p_{1/2})$	$(1p_{3/2})$	$(0f_{5/2})$	$(0f_{7/2})$	$(1d_{5/2})$	$(0g_{9/2})$
-0.055	-0.341	0.124	-0.716	0.118	-0.007

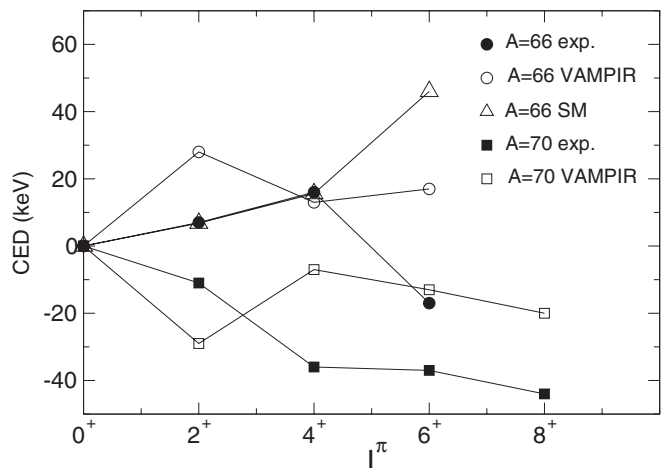


FIG. 5. Experimental CED (full symbols) for nuclei belonging to the  $A = 66$  and  $70$  isobaric multiplets. The experimental values are compared with the results of shell-model (open triangles) and excited Vampir (open circles and squares) calculations.

for the  $I^\pi = 2^+$  state of  $^{70}\text{Br}$  is  $Q_s = -6.4 e \text{fm}^2$  (prolate) and increases for higher spin (for  $I^\pi = 4^+$  and  $6^+$ ,  $Q_s = -9.8$  and  $-39.7 e \text{fm}^2$ , respectively). For the  $2^+$  and the  $4^+$  states in  $^{70}\text{Se}$ ,  $Q_s$  is equal to  $+4.5 e \text{fm}^2$  (oblate) and  $+11.5 e \text{fm}^2$  (oblate), respectively, turning to prolate values for increasing angular momentum (for  $I^\pi = 6^+$ ,  $Q_s = -17.5 e \text{fm}^2$ ). For the  $A = 66$  members of the isobaric multiplet, where new results are now available, shape competition is also observed, but here the ground state is found to be predominantly prolate in both nuclei. In  $^{66}\text{As}$ , the calculated oblate (prolate) components are 16% (84%), 29% (70%), 18% (81%), and 4% (95%) for the first  $0^+$ ,  $2^+$ ,  $4^+$ , and  $6^+$  states, respectively, whereas for the analog states in  $^{66}\text{Ge}$  the oblate (prolate) components are 20% (80%), 38% (61%), 32% (66%), and 9% (91%) for the corresponding states. The calculated spectroscopic quadrupole moments for the  $I^\pi = 2^+$  states of  $^{66}\text{As}$  and  $^{66}\text{Ge}$ ,  $Q_s = -11.4$  and  $-3 e \text{fm}^2$ , respectively, are both negative (prolate) and are increasing for higher spin.

In Fig. 5 the CED for nuclei belonging to the  $A = 66$  isobaric multiplet are compared with the results of the SM and of the excited Vampir calculations. The experimental CED show, as a function of spin, a slightly positive trend, becoming negative at  $I^\pi = (6^+)$ . Both theories (SM and excited Vampir) well reproduce the trend at low spin but predict a positive value for the  $(6^+)$  level. A negative trend of the CED is observed for  $A = 70$ . The energy differences between the predominantly prolate states of  $^{70}\text{Br}$  and the predominantly oblate states of  $^{70}\text{Se}$  result in a negative behavior of the  $A = 70$  CED, which is reasonably well reproduced by the calculation, although the detailed trend is not. The predominantly prolate states in the  $^{66}\text{As}$ - $^{66}\text{Ge}$  pair show smooth changes of the prolate-oblate mixing for increasing spin, which are reflected in the initially positive trend of the corresponding CED. A similar positive trend is observed experimentally for the  $^{82}\text{Nb}$ - $^{82}\text{Zr}$  and for  $^{86}\text{Tc}$ - $^{86}\text{Mo}$  pairs and is reproduced by our calculations, which in all cases suggest that prolate components dominate the yrast level sequences.

We conclude that the identified shape isomerism in  $^{66}\text{As}$  is consistent with the predicted coexistence of states with opposite sign of the quadrupole moment at low excitation energy. The mixing of oblate-prolate shapes strongly perturbs the isospin symmetry, altering the excitation energies of the levels in the nuclei of the same isospin multiplet, which is reflected in the CED behavior. For the  $^{70}\text{Br}$ - $^{70}\text{Se}$  pair this results in opposite ground-state deformation. The overall trend of the CED is reasonably well reproduced by the calculations even if we take into account only the isospin mixing determined by the Coulomb interaction. Deviations of the theoretical results from the experimental values indicate the need for a further increase in the dimension of the many-nucleon excited Vampir bases. Also, more experimental data are needed to track the CED behavior at higher spin as well as to extend the experimental systematics to the full isospin multiplets. Particularly useful in such a context would be the determination of the electromagnetic transition strengths and of the quadrupole moments of the analog states for the members of the isobaric multiplet.

## V. SUMMARY

In summary, the study of the excited states of the  $N = Z$  nucleus  $^{66}\text{As}$ , where a new  $3^+$  isomeric state has been identified

whose properties are consistent with the predicted oblate shape isomer, was used to investigate the coexistence of prolate-oblate deformations in different members of isobaric triplets in the  $A = 70$  mass region. The behavior of the CED is explained by different mixing of competing shapes in nuclei of the same isospin multiplet due to the effects of the isospin-breaking Coulomb interaction on the single-particle levels. Such a finding shows the crucial role played by shape coexistence phenomena in perturbing the isospin symmetry.

## ACKNOWLEDGMENTS

We thank the accelerator crew of Argonne National Laboratory for excellent support. This work was partly supported by Istituto Nazionale di Fisica Nucleare (I), the US Department of Energy under Contract No. DE-AC02-06CH11357 and Grant No. DE-FG02-88ER-40406, MICINN Spain Grant No. FPA2008-03774-E and the UK STFC. A. Gadea and E. Farnea acknowledge the support of MICINN, Spain, and INFN, Italy, through the AIC10-D-000568 bilateral action. A. Gadea has been partially supported by MICINN and Generalitat Valenciana, Spain, under Grants No. FPA2008-06419, No. FPA2011-29854, and PROMETEO/2010/101.

- 
- [1] M. A. Bentley and S. M. Lenzi, *Prog. Part. Nucl. Phys.* **59**, 497 (2007).
  - [2] A. Gadea *et al.*, *Phys. Rev. Lett.* **97**, 152501 (2006).
  - [3] B. S. Nara Singh *et al.*, *Phys. Rev. C* **75**, 061301(R) (2007).
  - [4] A. B. Garnsworthy *et al.*, *Phys. Lett. B* **660**, 326 (2008).
  - [5] R. Wadsworth *et al.*, *Acta Physica Polonica B* **40**, 611 (2009).
  - [6] J. Savory *et al.*, *Phys. Rev. Lett.* **102**, 132501 (2009).
  - [7] G. de Angelis *et al.*, *Eur. Phys. J. A* **12**, 51 (2001).
  - [8] I.-Y. Lee, *Nucl. Phys. A* **520**, c641 (1990).
  - [9] D. G. Sarantites *et al.*, *Nucl. Instrum. Methods Phys. Res., Sect. A* **381**, 418 (1996).
  - [10] D. G. Sarantites *et al.*, *Nucl. Instrum. Methods Phys. Res., Sect. A* **530**, 473 (2004).
  - [11] R. Grzywacz *et al.*, *Nucl. Phys. A* **682**, 41 (2001).
  - [12] R. Orlandi *et al.*, *Phys. Rev. Lett.* **103**, 052501 (2009).
  - [13] M. Hasegawa *et al.*, *Phys. Lett. B* **617**, 150 (2005).
  - [14] M. Honma, T. Otsuka, T. Mizusaki, and M. Hjorth-Jensen, *Phys. Rev. C* **80**, 064323 (2009).
  - [15] S. M. Vincent *et al.*, *Phys. Lett. B* **437**, 264 (1998).
  - [16] D. Rudolph *et al.*, *Phys. Rev. C* **69**, 034309 (2004).
  - [17] G. de Angelis *et al.*, *Eur. Phys. J. A* **12**, 51 (2001).
  - [18] S. M. Fischer, C. J. Lister, N. J. Hammond, R. V. F. Janssens, T. L. Khoo, T. Lauritsen, E. F. Moore, D. Seweryniak, S. Sinha, D. P. Balamuth, P. A. Hausladen, D. G. Sarantites, W. Reviol, P. Chowdhury, S. D. Paul, C. Baktash, and C.-H. Yu, *Phys. Rev. C* **74**, 054304 (2006).
  - [19] I. Schneider *et al.*, *Phys. Rev. C* **61**, 044312 (2000).
  - [20] A. F. Lisetskiy, R. V. Jolos, N. Pietralla, and P. von Brentano, *Phys. Rev. C* **60**, 064310 (1999).
  - [21] A. Petrovici *et al.*, *Nucl. Phys. A* **483**, 317 (1988).
  - [22] A. Petrovici *et al.*, *Nucl. Phys. A* **728**, 396 (2003).
  - [23] J. Ljungvall *et al.*, *Phys. Rev. Lett.* **100**, 102502 (2008).
  - [24] A. Petrovici *et al.*, *Nucl. Phys. A* **549**, 352 (1992).